Formation of one dimensional molybdenum oxide on Mo(112).

S. Kaya[1], J. Weissenrieder[1], D. Stacchiola[1], T. K. Todorova[2], M. Sierka[2], J. Sauer[2], S. Shaikhutdinov[1*], H.-J. Freund[1]

[1]*Fritz-Haber-Institut der Max-Planck-Gesellschaft, Faradayweg 4-6, 14195 Berlin, Germany*

[2]*Humboldt-Universität zu Berlin, Institut für Chemie, Unter den Linden 6, 10099 Berlin, Germany*

Abstract.

The atomic structure of a reconstructed Mo(112)-O(2x3) surface has been revisited using photoelectron spectroscopy with synchrotron radiation, scanning tunneling microscopy, infrared reflection absorption spectroscopy and density functional theory. In contrast to previous models, the results are rationalized in terms of the formation of one-dimensional, Mo=O terminated molybdenum oxide involving corner-sharing distorted [MoO_6] octahedra on the (1x3) reconstructed Mo(112) surface.

Keywords: molybdenum oxides; surface reconstruction; infrared spectroscopy; photoelectron spectroscopy; density functional theory.

* Corresponding author: *shaikhutdinov@fhi-berlin.mpg.de*

Introduction.

Understanding of oxygen induced reconstructions of metal surfaces is important in many technological fields such as corrosion, sensors, catalysis, etc. The initial stages of oxidation of metallic surfaces are generally believed to proceed through the formation of a chemisorbed oxygen layer, followed by nucleation and growth of oxide islands.

Adsorption of molecular oxygen and oxide formation on Mo surfaces have been the subject of a number of experimental and theoretical studies due to the use of molybdenum oxides as selective oxidation catalysts in industrially important catalytic processes[1-5]. Different surface structures have been observed on Mo(110), Mo(111) and Mo(100) surfaces depending on the oxygen coverage (Refs.(6-11) and references therein). A more open Mo(112) surface exhibits a ridge-and-trough structure (Fig. 1a), which provides several adsorption sites for oxygen: an on-top site, a short bridge site between two surface molybdenum atoms along the $[\bar{1}10]$ direction, a long bridge site, and finally two types of "quasi" three-fold hollow sites involving the topmost Mo atoms and those in troughs. Depending on experimental conditions, various surface structures have been reported for the Mo(112) surface such as (1×2), (1×3), (2×1), c(4×2), to name a few[12-14]. A (2x3) reconstructed surface was first observed by Schroeder et al. in the course of the preparation of thin silica films on Mo(112)[15-16]. The authors suggested the (2x3) surface to be a precursor to the formation of an epitaxial MoO_2 film [17-18]. However, Santra et al. proposed the (1x3) reconstructed Mo(112) surface to be the precursor to a MoO_2 film[14].

Monitoring the O/Mo(112) surface by X-ray photoelectron spectroscopy (XPS), Schroeder et al. concluded that the (2x3) surface reconstruction was induced by oxygen adsorption and not by oxidation [18]. Employing scanning tunneling microscopy (STM) and effective medium theory, the authors have proposed a model, where four oxygen atoms per (2x3) unit cell occupy on-top and "quasi" three-fold hollow sites on the missing-row type reconstructed Mo(112) surface, as shown in Fig. 1a. Note that the model of Santra et al. for the (1x3) surface also includes only adsorbed oxygen atoms [14].

Using density functional theory (DFT) Kiejna and Nieminen [19] recently showed that the short-bridge sites on the uppermost Mo rows are the most stable at lowest O coverage. For the (2x3) surface, the authors proposed another, more stable structure where the oxygen atoms occupy only quasi-threefold hollow sites, and suggested that the structure proposed by Schroeder et al. [17] is metastable. However, the authors did not consider the effect of oxygen partial pressure on the stability of different structures and assumed the same oxygen content as in the Schroeder at al's model. Our very recent DFT study [20] in combination with a genetic algorithm (GA) have predicted a high flexibility of the Mo(112) surface that easily undergoes a missing row type reconstruction in the oxygen environment. The GA simulations including effect of oxygen partial pressure yielded Mo(112)-O(1x2) and -O(1x3) structures more stable than all previously suggested models. These models were in a good agreement with experimental results [20] and in particular involved substantially more oxygen atoms in the unit cell than in the previous models.

In this work, using high resolution XPS with synchrotron radiation, STM and infrared reflection absorption spectroscopy (IRAS) in combination with DFT, we provide strong evidence that the O(2x3)-Mo(112) surface should be considered as Mo=O terminated one-dimensional molybdenum oxide consisting of rows of corner sharing distorted [MoO_6] octahedra.

2. Experimental.

The experiments were carried out in an UHV system equipped with ultraviolet and X-ray photoelectron spectroscopy (UPS/XPS Scienta SES 200), low energy electron diffraction (LEED, Omicron), scanning tunneling microscopy (STM, Omicron), and infrared reflection absorption spectroscopy (IRAS, Bruker 66ivs). The IRA-spectra in the 600 – 4000 cm^{-1} region (resolution ~ 2 cm^{-1}) were recorded at a grazing incidence (~84°) in specular geometry.

The Mo(112) single crystal (Mateck) was cleaned by repeated cycles of oxidation at 700 K and thermal flash to 2300 K until no contaminations were detected by XPS. The

(2x3) surface was formed by exposure to $5x10^{-8}$ mbar of O_2 (~ 800 L) at 850 K as judged by LEED.

The high-resolution photoelectron spectra were taken at BESSY II (beam line UE56/2-PGM1) using a Scienta R4000 analyzer. The binding energies (BE) for the Mo 3d and O 1s core levels were measured with a spectral resolution of ~ 100 and 200 meV, respectively, and referenced to the Fermi edge. Spectral deconvolution was performed using an asymmetric Lorentzian line profile convoluted with a Gaussian function. Shirley-type background was used for both normal and grazing emission spectra.

The computational setup for GA runs using DFT is analogous to the one described in Ref. 20. All calculations were performed using the Vienna Ab initio Simulation Package (VASP) [21-22] along with the Perdew-Wang exchange-correlation functional (PW91)[23]. The electron-ion interactions were described by the projector augmented wave (PAW) method [24] in the implementation of Kresse and Joubert [25]. We used a dual computational strategy for GA calculations. For initial runs a plane-wave basis set with an energy cutoff of 200 eV along with appropriate PAW potentials and a (2×2×1) Monkhorst-Pack grid [26] for the integration of the Brillouin zone were used. The final structure optimizations and energy evaluations of the atomic structure models resulting from the GA runs applied an energy cutoff of 400 eV and a (12×4×1) k-points grid.

For calculations of the vibrational spectra we used a central finite difference method, with intensities obtained from the derivatives of the dipole moment component perpendicular to the surface. To compensate for the systematic errors of DFT the frequencies were scaled by an empirical factor [27]. The factor of 1.00966 has been derived from comparison of experimental (1048 cm^{-1}) [28] and calculated harmonic (1038 cm^{-1}) frequencies for the Mo=O stretching vibration in $MoOF_4$.

The STM images are simulated from the self-consistent charge density employing the Tersoff-Hamann approach [29]. The core-level energies were calculated including final state effects using a modified projector augmented wave method within the Slater-Janak transition state approach [30].

3. Results and discussion.

The LEED pattern of the Mo(112)-(2x3)O surface is shown in Fig. 1b. While the unit cell spacing in the $[\bar{1}10]$ direction, i.e. three times that of the clean substrate, is quite obvious, the diffraction spots at half the reciprocal unit vector in the $[\bar{1}\,\bar{1}1]$ direction are streaky along the $[\bar{1}10]$ direction, indicating a high density of antiphase domain boundaries [17].

STM study of the (2x3) surface revealed the formation of stripes running in the $[\bar{1}\,\bar{1}1]$ direction (see Fig. 2). These stripes are often terminated with ill-defined structures forming step edges (henceforth referred to as "facets") as shown in Fig. 2b. That the original smooth surface of the clean Mo(112) becomes highly corrugated points to intense mass transport upon oxygen adsorption at elevated temperatures. High-resolution STM images, which are similar to those previously reported by Schroeder et al. [17,18] reveal domains consisting of zigzagged rows of protrusions in the $[\bar{1}\,\bar{1}1]$ direction separated by ~ 13.5 Å as shown in Fig. 2c. These domains are of different length along the $[\bar{1}10]$ direction (see Fig. 2b) and also include rows, which are shifted by half of a lattice in the $[\bar{1}\,\bar{1}1]$ direction, as indicated in Fig. 2c. The latter findings are consistent with streaky diffraction spots in LEED (see Fig. 1b).

The IRAS study of the (2x3) reconstructed surface revealed only two bands centered at 1024 and 1010 cm^{-1} (Fig. 3a). Frequencies around 1000 cm^{-1} are typical for Mo=O stretching vibrations as observed on the reference compounds and supported Mo catalysts [3,5,11,28,31-35]. The frequency of Mo=O species depends on the local coordination and may vary in the range of 1050 - 980 cm^{-1}.

It is noteworthy that the high frequency signal at 1024 cm^{-1} has lower intensity than the signal at 1010 cm^{-1}. This excludes the interpretation of these two peaks in terms of symmetric and asymmetric Mo=O stretching of di-oxo (O=Mo=O) species as well as any speculations on the "intensity borrowing" mechanism for a coupled, two dipole system with similar individual frequencies (e.g., see [36]); both models lead to a higher intensity of higher frequency vibrations. In addition, the isotopic experiments with O^{18} (Fig. 3b) show the same two bands only red-shifted to 975 and 962 cm^{-1} with no changes in the intensity ratio and relative peak position otherwise expected for di-oxo species [31].

Finally, the intensity ratio of the two bands depends on preparation. The high frequency peak gains intensity upon increasing the oxidation temperature from 850 to 1000 K. STM inspection of the samples prepared at the higher oxidation temperature showed a higher degree of faceting. When prepared at 850 K, these features typically cover 10 - 15 % of the entire surface, i.e. close to the intensity ratio of I_{1024}/I_{1010} in the IRA spectrum. Note that the similar vibrational properties have been observed by Nart et al. [11] on oxidized Mo(110) surfaces and were attributed to Mo=O moieties on terraces and steps, respectively. Therefore, we conclude that the terraces with a (2×3) structure seen in STM expose mono-oxo (Mo=O) species.

Figure 4 shows high resolution Mo 3d photoelectron spectra of the Mo(112)-(2×3)O surface measured at normal and grazing electron emission angles. At least five different $Mo^{+\delta}$ states beyond the metallic state at 228.0 eV are resolved. The observation of the highest BE states is partially obscured due to overlapping with $3d_{3/2}$ spin-orbit components of the low BE states, but their presence is clearly seen at the grazing emission. In the following text, we will only refer to the $3d_{5/2}$ spin-orbit components in the spectra for simplicity. Table 1 presents the BE values and relative intensity of each Mo state found in the deconvoluted spectra, although the accurate position of the high BE states is rather uncertain.

Comparing the relative signal intensity at normal and grazing emission, one can see that the metallic state at 228.0 eV and partially oxidized state at 228.45 eV attenuate at grazing emission and are therefore associated with “bulk” or “sub-surface” species. (Note that the escape depth of the Mo 3d photoelectrons at excitation energy $h\nu$ = 330 eV used in these experiments corresponds to 3-4 atomic layers, on average). Meanwhile, the signals at higher BEs gain the intensity at the grazing emission thus indicating the “surface” nature of these species.

The O 1s spectra (not shown here) exhibit a broad peak (FWHM > 2 eV) centered around 530 eV with a pronounced asymmetry at the high energy side, indicating the presence of oxygen atoms in different chemical environments, although the states could not be precisely resolved and deconvoluted as for the Mo 3d level. Nevertheless, the O 1s signal was used to calibrate the amount of oxygen on the (2x3) surface by comparison with the spectra of an ultra-thin silica film grown on the same Mo(112) substrate, for

which the atomic structure has recently been determined [37, 38]. This gave us an oxygen coverage of about 0.15 O-atoms/Å^2 in the p(2×3) structure or approximately 11 oxygen atoms per (2×3) unit cell. This amount of oxygen is much higher than in the previously proposed model with only 4 O atoms in the cell [17, 18]. Therefore, the XPS results clearly indicate an O-rich structure of the O(2x3)-Mo(112) surface.

The observation of a large variety of differently coordinated Mo and O atoms basically discards the surface structures with only chemisorbed oxygen and allows us to consider the formation of Mo oxide structures. Certainly, structural differences that are expected for the surface and bulk oxides make direct comparison of the corresponding XPS data precarious. For example, the peaks at 229.5 and 234.2 eV were reported for the Mo $3d_{5/2}$ and $3d_{3/2}$ levels in MoO_2, respectively [39, 40]. The MoO_3 films grown on Au(111) show states around 232.5 and 235.8 eV, respectively [41]. In addition, the determination of the Mo oxidation state in non-stoichiometric oxides is not straightforward due to screening effects, which are expected to be different for conductive MoO_2 and insulating MoO_3. Indeed, enhanced core-hole screening has been reported for metallic $K_{0.3}MoO_3$ bronze [42]. In the case of ultra-thin oxide films, additional screening by a metal substrate underneath the film may result in lowering of the measured BE values. Taking all this into account and using the XPS data presented in Fig. 4 and Table 1, we conclude that a significant fraction of the Mo atoms in the (2x3) structure is in the oxidation state above 4+. Again, this situation cannot be rationalized in terms of the solely chemisorbed oxygen.

Thus, the key observations for the Mo(112)-(2x3)O surface can be summarized as follows: (i) at least five differently oxidized Mo atoms are present in the structure; (ii) the structure includes surface Mo=O species; (iii) a high oxygen content (approximately 11 O atoms) are in the (2x3) unit cell; (iv) zigzagged rows are observed in STM images.

As a starting point of structure modeling, we have to recall that the Mo atoms in the Mo oxides follow tetrahedral or octahedral coordination to oxygen. In principle, the Mo=O species are present only in the MoO_3 phase, which consists of layers of slightly distorted [MoO_6] octahedra. Note also that for surface metal oxygen double bond species STM displays the oxygen atoms as protrusions when probing the occupied states which are constituted basically of O2p (e.g., see [43]). Therefore, we may assign the rows of

zigzagged protrusions seen in STM to the outmost O atoms of the Mo=O bonds in [MoO_6] octahedra. Alternatively, the Mo atoms on the surface can be five-fold coordinated as O=MoO_4. To fit STM images, the [MoO_6] octahedra or O=MoO_4 pyramids can be arranged in a zigzagged line through corner sharing in the [MoO_4] plane with the Mo=O bonds pointing out of the surface. Putting aside for the moment the details of bonding and simply placing the zigzagged rows on top of the Mo(112)-(1x3) surface (to accomplish the (2x3) symmetry of the whole structure) will result in 7 and 9 oxygen atoms per (2x3) cell for five-fold and six-fold coordinated Mo atoms in the unit block, respectively. Both these numbers are still below the 11 O atoms measured by XPS. Therefore, additional O atoms must be included in the structure.

A genetic algorithm was further employed to determine thermodynamically the most stable (2x3) surface in the same manner as previously used for O(1x2)- and O(1x3)-reconstructed Mo(112) [20]. The most stable structure found with GA is shown in Fig. 5. This structure accommodates 13 oxygen atoms and involves corner-sharing [MoO_6] octahedra along the $[\bar{1}\,\bar{1}\,1]$ direction. In agreement with the STM image shown in Fig. 3b, the simulated image shows the protruding zigzagged rows, where the protrusions are assigned to the O atoms of Mo=O bonds.

In this model, one can discriminate five differently coordinated to oxygen Mo atoms (labeled 1-5 in Fig. 5) as experimentally observed by XPS. In order to validate the model, we have calculated binding energies of the Mo $3d_{5/2}$ level for each Mo atom in the unit cell. Due to the limitations of our computational model we used the Mo atom (6) in Fig. 5 as the reference for the metallic state. The results are summarized in the Table 2, where the BE shifts with respect to the metallic state are shown for clarity. In the first approximation, we also assumed that the signal intensity is proportional to the number of each Mo species. The calculations are fairly consistent with experimental data and show five types of Mo atoms in different oxidation states, with the highest BE shift for the Mo atom coordinated to six O atoms (1 in Fig 5). Also, the calculated BE shifts consistently decrease with decreasing number of coordinated O atoms, almost reaching the BE of metal for the Mo atoms (4,5) in the troughs of the (1x3) reconstructed Mo surface. Note, however, that the comparison between calculated and experimental XPS results may be

hampered by the presence of “facets” (see Fig. 2b), the coverage of which could not be precisely controlled in the XPS experiments.

Harmonic frequency calculations for the model shown in Fig. 5 yield only two IRAS active vibrational modes above 600 cm^{-1} (the lower limit for experiments), namely at 1007 and 1005 cm^{-1}, with an intensity ratio about 60 : 1. These two vibrations belong to in and out of phase stretching vibrational couplings, respectively, of the Mo=O groups of octahedrally coordinated Mo atoms in the (2x3) unit cell. The calculated frequency is in excellent agreement with the experimentally observed 1010 cm^{-1} (Fig. 3). Therefore, the band at 1024 cm^{-1} must be assigned to the ill-defined “facets”, which probably reflects an initial stage of the formation of a MoO_2 thin film [18].

4. Summary.

In this work, we have studied the structure of oxygen induced (2x3) reconstruction on the Mo(112) surface using high resolution XPS with synchrotron radiation, STM, IRAS and DFT. The results reveal a more complex structure of the reconstructed surface than previously proposed. The experimental results cannot be explained on the basis of only surface oxygen. Based on a combination of experimental results and DFT calculations using a genetic algorithm, we propose the model involving a Mo=O terminated, one-dimensional Mo oxide structure, formed through corner sharing of $[MoO_6]$ octahedra adsorbed on the (1x3) reconstructed Mo(112) surface.

Acnowledgements.

The authors gratefully acknowledge financial support by Deutsche Forschungsgemeinschaft (DFG) through SFB 546 and the Fonds der Chemischen Industrie. S.K. and T.K.T. acknowledge the International Max Planck Research School “Complex Surfaces in Materials Science” for fellowships. D.S. and J.W. thank the Alexander von Humboldt Foundation for fellowships. The calculations were carried out at the Norddeutscher Verbund für Hoch- und Höchstleistungsrechnen (HLRN).

References.

1. J. Haber, *Molybdenum: an outline of its chemistry and uses,* in *Studies in inorganic chemistry,* Vol. 19; E. R. Braithwaite, J. Haber (Eds); Elsevier, 1994.
2. Y. Iwasawa, Adv. Catal. 35 (1987), 187.
3. J.M.Jehng, H.C. Hu, X.T. Gao and I.E. Wachs, Catal. Today, 28 (1996), 335.
4. K.D.Chen, A.T. Bell and E. Iglesia, J. Catal. 209 (2002), 35.
5. G. Mestl and T.K.K. Srinivasan, Catal. Rev. - Sci. Eng. 40 (1998), 451.
6. I.K. Robinson, D.-M. Smilgies and P.J. Eng, J. Phys. Condens. Matter, 4 (1992), 5845.
7. H. Xu and K.Y.S. Ng, Surf. Sci. 356(1996), 19.
8. J. Kröger, T. Greber and J.Osterwalde, Surf. Sci. 459 (2000), 173.
9. A. Okada, M. Yoshimura and K. Ueda, Surf. Sci. 601(2007), 1333.
10. P.K. Stefanov and T.S. Marinova, Surf. Sci. 200 (1988), 26.
11. F.C. Nart, S. Kelling and C.M. Friend, J. Phys. Chem. B 104 (2000), 3212.
12. T. Sasaki, Y. Goto, R.Tero, K. Fukui and Y. Iwasawa, Surf. Sci. 502 (2002), 136.
13. K. Fukui, T. Aruga and Y. Iwasawa, Surf. Sci. 281 (1993), 241.
14. A.K. Santra, B.K.Min and D.W. Goodman, Surf. Sci. Lett., 513 (2002), L441.
15. T. Schroeder, M. Adelt, B. Richter, M. Naschitzki, M. Bäumer and H.-J. Freund, Surf. Rev. Lett. 7 (2000), 7.
16. T. Schroeder, J.B. Giorgi, M. Bäumer and H.-J. Freund, Phys. Rev. B 66 (2002), 165422.
17. T. Schroeder, J.B. Giorgi, A. Hammodeuh, N. Magg, M. Bäumer, H.-J. Freund, Phys. Rev. B, 65 (2002), 115411.
18. T. Schroeder, J. Zegenhagen, N. Magg, B. Immaraporn and H.-J. Freund, Surf. Sci., 552 (2004), 85.
19. A. Keijna and R.M. Nieminen, J. Chem. Phys. 122 (2005), 044712.
20. M. Sierka, T.K. Todorova, J. Sauer, S. Kaya, D. Stacchiola, J. Weissenrieder, S. Shaikhutdinov and H.-J. Freund, J. Chem. Phys. 126 (2007), 234710.
21. G. Kresse and J. Furthmüller, Comput. Mater. Sci. 6 (1996), 15.
22. G. Kresse and J. Furthmüller, Phys. Rev. B 54 (1996), 11169.

23. J. P. Perdew, J. A. Chevary, S. H. Vosko, K. A. Jackson, M. R. Pederson, D. J. Singh and C. Fiolhais, Phys. Rev. B 46 (1992), 6671.
24. P. E. Blöchl, Phys. Rev. B 50 (1994), 17953.
25. G. Kresse and D. Joubert, Phys. Rev. B 59 (1999), 1758.
26. H. J. Monkhorst and J. D. Pack, Phys. Rev. B 13 (1976), 5188.
27. J.F. Scott and S.P.S. Porto, Phys. Rev. 161 (1967), 903.
28. L. E. Alexander, I. R. Beattie, A, Bukovszky, P. J. Jones, C. J. Marsden and G. J. Van Schalkwyk, J. Chem Soc., Dalton Trans. 81 (1974).
29. J. Tersoff and D.R. Hamann, Phys. Rev. Lett. 50 (1983), 1998.
30. J. C. Slater, in *Quantum Theory of Molecules and Solids*, vol.4 (McGraw-Hill, New York, 1974).
31. S. Chemath, Y. Zhang and A.T. Bell, J. Phys. Chem. C 111 (2007), 1291.
32. S. Razi Seyedmonir, S. Abdo and R.F. Howe, J. Phys. Chem. 86 (1982), 1233.
33. F.A. Cotton and R.M. Wing, Inorg. Chem. 4 (1965), 867.
34. M.A. Py and K. Maschke, Physica B, 105 (1985), 370.
35. S.-Y. Quek, M.M. Biener, J. Biener, C.M. Friend and E. Kaxiras, Surf. Sci. Lett. 577 (2005), L71.
36. P. Hollins, Surf. Sci. Rep. 16 (1992), 51.
37. J. Weissenrieder, S. Kaya, J.-L. Lu, H.-J. Gao, S. Shaikhutdinov, H.-J. Freund, M. Sierka, T. K. Todorova and J. Sauer, Phys. Rev. Lett. 95 (2005), 076103.
38. S. Kaya, M. Baron, D. Stacchiola, J. Weissenrieder, S. Shaikhutdinov, T. K. Todorova, M. Sierka, J. Sauer, and H.-J. Freund, Surf. Sci. 601 (2007), 4849.
39. T. Jirsak, M. Kuhn and J.A. Rodriguez, Surf. Sci. 457 (2000), 254.
40. J.F. Moulder, W. F. Stickle, P. E. Sobol and K. D. Bomben, *Handbook of X-ray Photoelectron Spectroscopy* (Perkin-Elmer Corporation USA, 1992).
41. M. Cavalleri, K. Hermann, S. Guimond, Y. Romanyshyn, H. Kuhlenbeck and H.-J. Freund, Catal. Today 124 (2007), 21.
42. Sing, R. Neudert, H. von Lips, M.S. Golden, M. Knupfer, J. Fink, R. Claessen, J. Mucke, H. Schmitt, S. Hufner, B. Lommel, W. Assmus, C. Jung and C. Hellwig, Phys. Rev. B 60 (1999), 8559.

43. R.-P. Blum, H. Niehus, C. Hucho, R. Fortrie, M.V. Ganduglia-Pirovano, J. Sauer, S. Shaikhutdinov and H.-J. Freund, Phys. Rev. Lett. 99 (2007), 226103.

Table 1. Binding energy and relative intensity of the Mo $3d_{5/2}$ signal in the deconvoluted XP-spectra shown in Fig. 4.

BE, eV	228	228.45	228.8	229.4	231.1	232.0
Intensity, (normal)	35	24	15.5	2.5	15	8
Intensity, (grazing)	18	19.5	19	9.5	20.5	13.5

Table 2. Binding energy and relative intensity of the experimental (at grazing emission) and calculated XP-spectra for the Mo $3d_{5/2}$ level. Numbers in parenthesis indicate the atom position as labeled in Fig. 5.

ΔBE (eV)	0.4	0.8	1.4	3.1	4.0	Exp.
Intensity	1	1	0.5	1	0.7	
ΔBE (eV)	~0 (4&5)	0.3 (*3*)	1 (2)	2.6 (*1*)		Calc.
Intensity	1	1	0.3	0.3		

Figure captions.

Figure 1. (a) Perspective view of Mo(112). (b) LEED pattern of O(2x3)-Mo(112) surface. (c) Model of the Mo(112)-(2x3)O surface proposed in Ref. 17. (White, light gray and dark gray circles represent Mo atoms in the first (protruding), second and third layers, respectively. Oxygen atoms are shown as small black circles.

Figure 2. STM images of the O(2x3)-Mo(112) surface. Size and tunneling parameters are (a) 40 × 40 nm^2, V= 1.0 V, I= 0.2 nA; (b) 50 × 50 nm^2, 1 V, 0.18 nA; (c) 9 × 9 nm^2, 1.2 V, 0.6 nA. The formation of "facets" terminating the (2x3) stripes is seen in (b). A (2x3) mesh is indicated in (c) to highlight two stripes that are shifted by half of a lattice in the $[\bar{1}\,\bar{1}\,1]$ direction.

Figure 3. IRA spectra of the Mo(112)-(2x3)O surface prepared with O^{16} and O^{18}.

Figure 4. Photoelectron spectra of the Mo 3d core level measured for the Mo(112)-(2x3)O surface at normal and grazing emission angles together with the deconvolution (see the text). Note that the highest BE states of Mo $3d_{5/2}$ are obscured due to overlapping with $3d_{3/2}$ spin-orbit components of the low BE states.

Figure 5. Cross and top views of the structural model of the reconstructed Mo(112)-(2x3)O surface. Simulated STM image is overlapped with the top view to highlight STM protrusions coming from the outermost oxygen atoms of the M=O bonds.

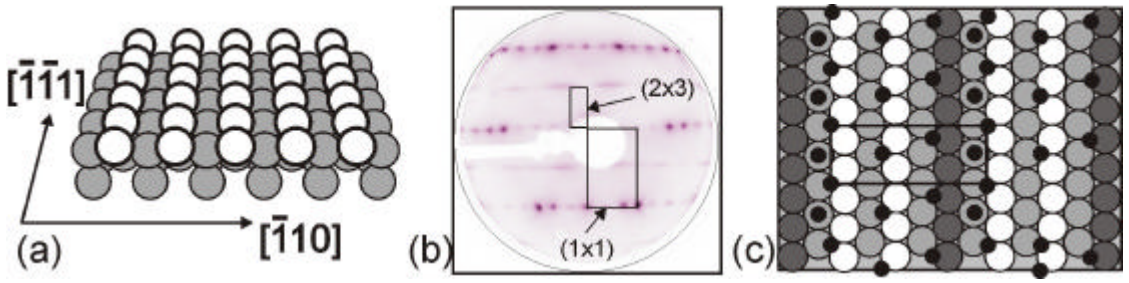

Fig. 1

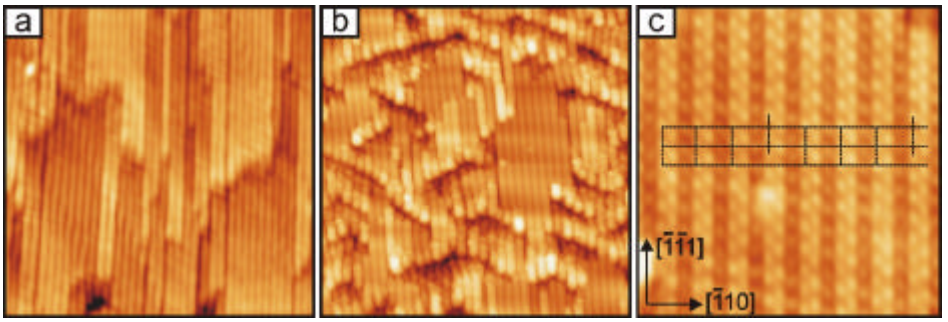

Fig. 2

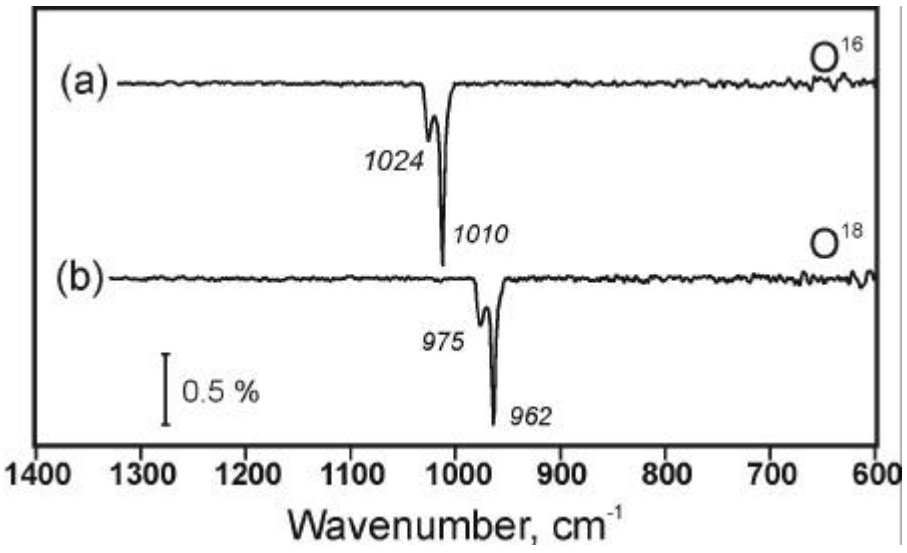

Fig. 3

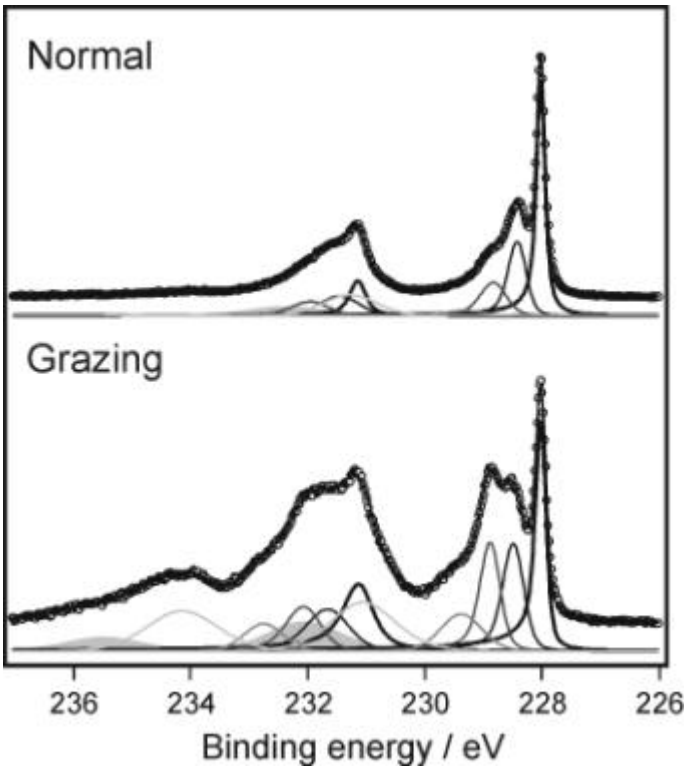
Normal
Grazing
236
234
232
230
228
226
Binding energy / eV

Fig. 4

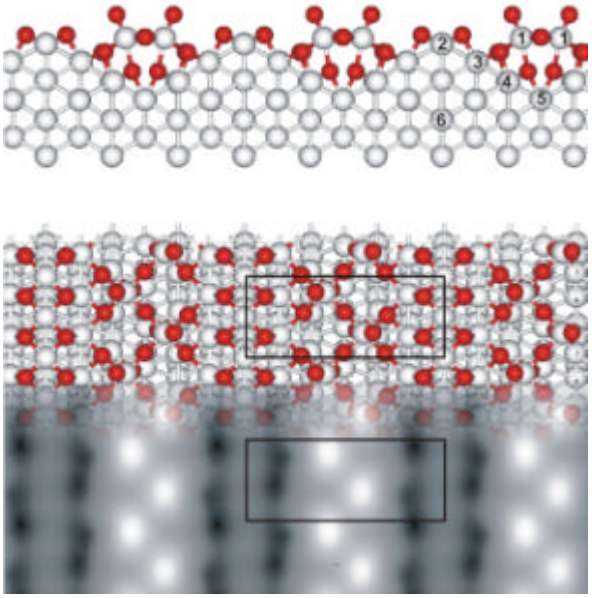
1
1
2
3
4
5
6

Fig. 5